Study of Coal Gasification in an Experimental Fluidized Bed Reactor

Thermal gasification has been proposed as one technical option for the conversion of coal to gaseous fuels and/or chemicals to supplement supplies presently derived from petroleum and natural gas. In the present study, a bench-scale fluidized bed reactor was used for the gasification of coal with steam as the fluidizing medium. A mixture of sand and limestone used as the bed material made it possible to gasify a caking coal without the problem of agglomeration. The gas composition and yield of the hydrogen-rich product gas were studied as a function of temperature.

To study the heterogeneous reactions taking place in the reactor and also the transient behavior of the system, a mathematical model was developed. The model assumed a reaction mechanism that accounted for the devolatilization of coal, cracking of volatiles, char gasification, and the water-gas shift reaction. Both the dynamic behavior and steady state performance of the gasifier were simulated based on the model. The steady state results of the simulation were compared with the experimental data. This comparison enabled us to ascertain that the proposed reaction mechanism and dynamic model predicted the correct trends.

D. NEOGI, C. C. CHANG, W. P. WALAWENDER, and L. T. FAN

Department of Chemical Engineering
Kansas State University
Manhattan, KS 66506

SCOPE

Conversion of the nation's vast resources of coal to liquid and gaseous fuels has been envisioned as a major contribution to the energy picture in the future. Several feasible conversion processes have been proposed; among them is fluidized bed gasification. Although many contacting devices have been proposed for coal gasification, fluidized beds are widely used because of their advantageous characteristics, such as high rates of heat transfer and excellent gas-solid contacting. Even though numerous experimental studies on fluidized bed coal gasification have been undertaken, relatively little has been done to model it.

A mathematical model incorporating the dominant mechanistic features has been developed to describe the gasification of coal in a fluidized bed reactor. The model does not include the initial devolatilization because that is considered to proceed nearly instantaneously; it includes only the secondary reactions. The governing equations of the model, a set of partial differential equations (PDE), have been solved by an existing PDE software package for simulation.

A series of gasification runs was conducted with a bench-scale fluidized bed reactor to obtain experimental data for comparison with the model.

CONCLUSIONS AND SIGNIFICANCE

A dynamic model has been developed to study coal gasification in a fluidized bed reactor. Based on the model, the transient and steady state behavior of the gasifier were simulated. The simulated steady state results compare favorably with the experimental results obtained from the gasification of coal in a bench-scale fluidized bed reactor. More specifically the model correctly predicts the trends in the gas composition, overall mass yield of the product gas and mass yields of the individual gas components, and the amount of char produced. Among the model refinements suggested are inclusions of tar cracking reactions, and enhancement of the data base for the initial devolatilization and char gasification reactions.

INTRODUCTION

Fluidized bed gasification has been proposed as a process for converting coal, biomass, and waste materials into fuel gas. It is well known that the scale-up, design, operation, and control of any process are vastly facilitated by the availability of a mathematical model; fluidized bed gasification is no exception. Modeling this process requires a knowledge of the hydrody-

namics and chemical phenomena that take place in the bed. Also, any mathematical model developed must be verified experimentally before it can be implemented in practice.

Zeles (1978) presented a mathematical model for the simulation of steam-oxygen gasification of coal in a fluidized bed. A modification of the bubble assemblage model (Kato and Wen, 1969) was used to model the fluidized bed. Kinetic expressions for the reactions of carbon with O_2, H_2O (steam), H_2, and CO_2 were used for the emulsion and cloud phases. Simulated results, based on the model, compared favorably with the experimental data obtained by the Institute of Gas Technology (Zeles, 1978). The experiments were conducted in a 15.24 cm dia. fluidized bed reactor at pressures from 2,532,500 to 4,052,000 N/m^2. Elutriation and entrainment of char were not incorporated in this model. Lack of data on the rate of formation of individual volatile species made treatment of devolatilization difficult. The model was simplified substantially by the assumption that gas composition was independent of temperature. Dynamic characteristics of the gasification reactor were not studied; only steady state results were presented.

Biba et al. (1978) modeled the gasification of coal under pressure in a fixed bed reactor. Their paper focused on the parameters of reaction kinetics and on the transfer of material and energy that were necessary for developing the model of the fixed bed reactor. The resultant system of differential equations was solved in order to calculate the concentration and temperature profiles in the solid and gas phases as a function of the bed height. Only the steady state behavior of the reactor was considered in their work.

A model for the fluidized bed combustion of coal was presented by Becker et al. (1975). The material and energy balances for coal combustion were considered and models were developed for various terms in these balances. Both steady state and transient operations were studied; however the governing equations of the model were not solved, and thus no comparison was made with experimental data to prove its validity.

A steady state model of the moving bed coal gasifier was developed by Yoon et al. (1977), based on kinetics and transport rate processes, thermodynamic relations, and mass and energy balances. Model predictions were in good agreement with published plant data for the Lurgi gasifier.

Recently, Raman et al. (1981) presented a model to describe the fluidized bed gasification of biomass and applied it to the gasification of feedlot manure. Several simplifying assumptions were imposed in deriving the model, and only steady state solutions were obtained. Chang et al. (1984) extended this work and considered the dynamic modeling of biomass gasification.

The objectives of the work reported here were:

1. To gasify coal in an experimental fluidized bed reactor.
2. To develop a mathematical model describing the process.
3. To simulate the dynamic characteristics of the reactor.
4. To obtain experimentally steady state performance data and compare them with the simulated steady state predictions from the model.

EXPERIMENTAL

Facilities

The fluidized bed reactor used in this work was designed to study pyrolysis and gasification of various carbonaceous materials, e.g., coal, at atmospheric pressure and over a temperature range of 650 to 1,450 K. The experimental system, shown in Figure 1, consisted of three primary sections: the reactor section, the gas clean-up section, and the gas sampling and analysis section. Construction details for the reactor are shown in Figure 2.

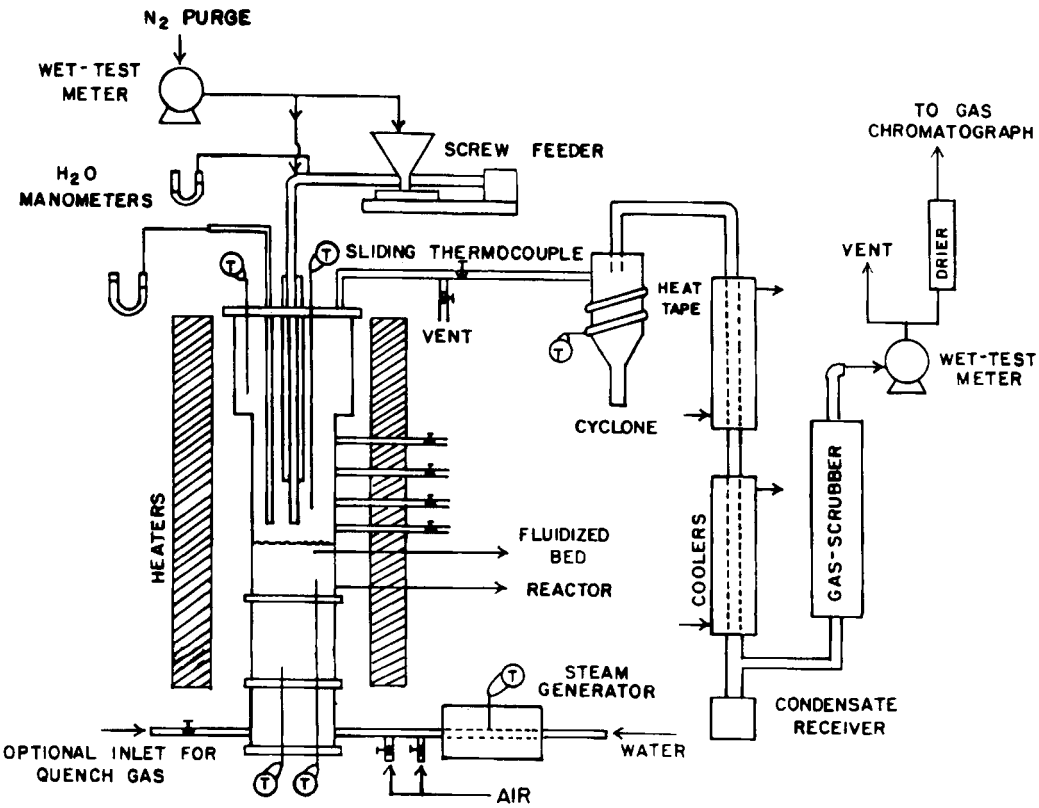

Figure 1. Bench-scale fluidized bed coal gasification system.

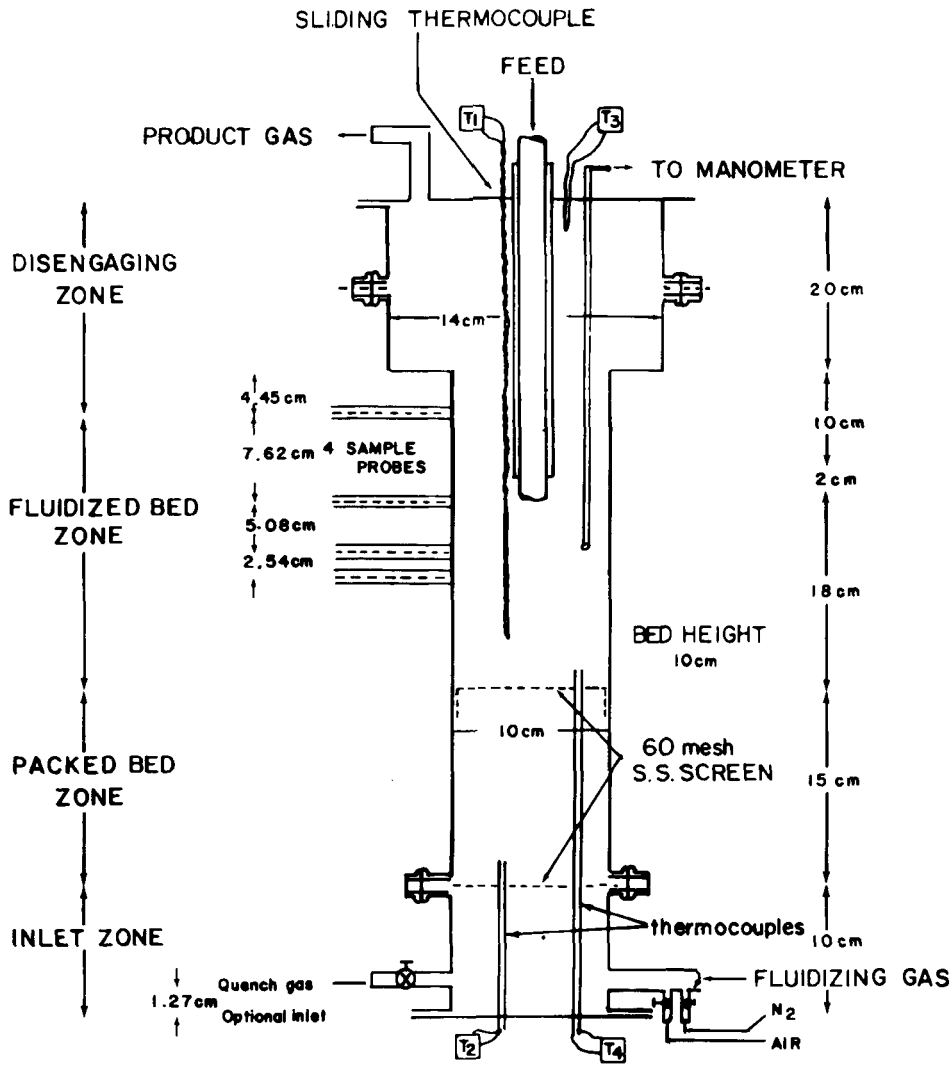

Figure 2. Fluidized bed reactor.

The inert matrix used for the bed material was composed approximately of a mixture of 25% by weight of limestone and 75% by weight of silica sand. The limestone was used to prevent bed agglomeration, which typically occurs in a bed composed solely of silica sand (Walawender et al., 1981). The limestone particle size was $2.82-0.287 \times 10^{-3}$ m; the sand particle size was $0.595-0.297 \times 10^{-3}$ m. The static bed height ranged from 0.08 to 0.1 m.

The reactor was heated by means of ten quarter-cylindrical electrical resistance heaters, each capable of delivering up to 1,200 watts of power with a maximum sustained operating temperature of 1,500 K. Voltage to each of them was controlled by PID controllers. There were five chromel alumel type thermocouples installed in the reactor. One, a sliding thermocouple, was used to measure the temperature profile inside the reactor. The others were located in the freeboard, the fluidized bed section, the preheating zone, and the middle of the reactor. Controllers recorded the temperatures from these thermocouples and accordingly activated the heaters as required to maintain the temperature in the reactor at a preset value. A pressure probe, connected to a manometer, indicated the bed pressure and the state of fluidization.

The feed was introduced into the reactor by gravity flow through a vertical feedpipe (0.03 m I.D.) which discharged at a location about 0.08 m above the static bed. A vibrating screw feeder was used to supply the feed at a uniform volumetric rate. A purge stream of nitrogen aided solid flow through the feedpipe and prevented gas backflow and subsequent condensation of vapor in the feeder. The flow rate of nitrogen was measured by a wet test meter. To prevent the feed materials from prematurely devolatilizing before reaching the bed (and possibly clogging the feedpipe in the process), the feedpipe was equipped with a water jacket that maintained the temperature inside the feedpipe below 400 K. Steam, the sole fluidizing gas, was produced externally in an electric boiler.

The gas exiting from the reactor was passed through a well-insulated cyclone which removed the elutriated solid particles, e.g., char, from the gas stream. After leaving the cyclone the gas stream passed through two water-cooled, double-pipe heat exchangers in series. This resulted in condensation of steam and tar, which were collected in a condensate receiver. Further gas cleaning was achieved by means of a dry scrubber packed with glass wool. This device was effective in removing the mist suspended in the gas with little pressure drop. A wet test meter connected to a strip chart recorder measured the flow rate of the gas. A side draw of the off-gas was passed through a drying column and then sent to an on-line process gas-chromatograph for analysis. The remaining gas was vented to the atmosphere. Nitrogen in the product gas, acting as a tracer, allowed computation of the rate of product gas generation, which was used for comparison with the wet-test meter readings.

Procedure

For start-up of each experimental run, the reactor heaters and steam generator were turned on and the controllers were set at the desired operating temperatures. During the heat-up period, air served as the

fluidizing agent and as the feed pipe purge gas; the water flow to the feedpipe jacket was turned on to cool the feedpipe. The steam generator was set to supply steam at constant pressure. Once steam was available, the fluidizing air flow was gradually replaced by steam. The volumetric flow rate of steam required to maintain fluidization was measured by collecting condensate downstream from the heat exchangers, and was controlled by a needle valve on the steam line.

When the bed and the freeboard reached the selected operating temperature, the axial temperature profile was measured, and if necessary minor corrections were made by adjusting the controllers to ensure a uniform temperature profile. The off-gas from the system was analyzed to insure that the system was free of air. At this point, the system was ready for feeding to begin. Total start-up time was about two hours from a cold start and about one hour from a warm start. Normally, at the end of each run the heaters were not turned off but just turned down so that the system stayed warm overnight.

A slight drop in the temperature of the reactor occurred when feeding was initiated, but was corrected automatically by the controllers. A gas sample was taken about 5 min after the initiation of feeding and every 11 min thereafter. Condensate and nitrogen flow rates were measured every 10 min throughout the run. A typical experiment at a given temperature lasted 100 to 120 min with the last 50 to 60 min yielding steady gas chromatograph readings. The feed rate of solids was measured by disconnecting the lower section of the feedpipe and weighing the effluent collected over three 3 min time intervals. This was carried out both at the start and end of the run.

It was not possible to directly measure the total char produced in an experiment run because of the holdup of char in the system. However ash balances were made, and by assuming that all the ash present in the feed appeared in the char, the amount of char produced was estimated.

It also was not possible to measure the total tar produced due to lack of adequate separation facilities; in addition, significant quantities of tar were held up in the heat-exchangers. Consequently, overall material balances were not attempted.

The operating conditions used in the experiments are summarized in Table 1. By adjusting the steam rate with the temperature of the run, an attempt was made to maintain a fairly constant mean residence time for the volatiles for all the runs. The gas phase mean residence time ranged from 4 to 7 s. The gas residence time was estimated on the basis of the reactor temperature, total dry gas flow rate, and steam rate. The steam rate was varied from 0.920 to 0.660 kg/h. The average feed rate was 0.312 kg/h. The principle experimental variable was the reactor temperature. All the experiments were performed with the temperature of the freeboard being the same as in the fluidized bed section, resulting in a uniform axial temperature profile. The range of temperature studied was from 823 to 1,133 K.

Chemical Analyses

Analysis of the dry off-gas was conducted with an on-line process gas chromatograph on an 11 min cycle. The measured components were H_2, CO, CO_2, CH_4, C_2H_4, C_2H_6, C_3H_6, C_3H_8, O_2, and N_2. No H_2S was detected in the product gas even though the feed coal contained 7.5 wt % of sulfur on dry ash free basis. This may be attributed to absorption of H_2S by the limestone present in the bed and the reaction of H_2S with iron, which was the material of construction of the reactor and the connecting pipes. Moisture and ash analyses of feed material were performed according to standard ASTM procedures. Elemental analysis of the feed was conducted with a Perkin-Elmer (Model 240B) Elemental Analyzer.

Feed Material

The material used for the gasification experiments was bituminous coal from the Rowe coal bed in southeast Kansas. The feed had a mean particle size of 2.97×10^{-4} m. The proximate and ultimate analyses of the coal are given in Table 2.

MODEL DEVELOPMENT

Gasification of coal in a fluidized bed reactor involves chemical reactions, as well as mass transport, that are profoundly affected by hydrodynamics in the reactor. The present model is based on the two-phase theory of fluidization with the following assumptions (Davidson and Harrison, 1963).

1. The fluidized bed consists of two phases, namely, bubble and emulsion phases, which are homogeneously distributed statistically.
2. The flow of gas in excess of the minimum fluidization velocity passes through the bed in the form of bubbles that are free of solids.
3. The voidage of the emulsion phase remains constant and is equal to that at incipient fluidization.
4. The bed can be characterized by an equivalent bubble size, and the flow of gas in the bubbles is in plug flow.
5. The emulsion phase is well mixed.
6. The bed is isothermal.
7. No reaction takes place in the freeboard of the reactor.
8. No tar cracking reactions take place in the reactor.

TABLE 1. OPERATING CONDITIONS OF THE EXPERIMENT

ε_{mf}	= 0.43
U_{mf}	= 0.12 – 0.09 m/s
B	= 0.973 kg
ρ	= 2,608 kg/m^3
A_c	= 200,000 m^2/kg
Feed rate	= 0.00007289 (DAF kg/s)
U_o	= 0.165 – 0.14 m/s
D_{ib}	= 0.001 m^2/s
D_{ie}	= 1,000 m^2/s
T	= 873–1,073 K
Mean coal particle size = 0.297 mm	
Composition of fluidizing gas, H_2O (steam) = 100%	
Steam rate = 15.33–11.0 g/min	
Steam consumption rate	
0.15 g/min at 873 K	
0.70 g/min at 923 K	
1.89 g/min at 973 K	
2.87 g/min at 1,033 K	
3.62 g/min at 1,073 K	

Chemical Reactions and Expressions of Rate Terms

In our previous studies (Howell, 1979; Raman et al., 1981; Chang et al., 1984), we have visualized that the gasification of coal or any carbonaceous material takes place in three steps:

(1) Coal $\xrightarrow{\text{devolatilization}}$ Heavy volatiles + Gas (CO_2, H_2, CO, CH_4, etc.) + Char

(2) Heavy volatiles $\xrightarrow{\text{cracking}}$ Liquid + gas

(3) Char gasification reactions:

$$C + H_2O \xrightarrow{k_1} CO + H_2$$
$$C + CO_2 \xrightarrow{k_2} 2CO$$
$$C + 2H_2 \xrightarrow{k_3} CH_4$$

Water-gas shift reaction $CO + H_2O \underset{k_5}{\overset{k_4}{\rightleftharpoons}} CO_2 + H_2$

The first step in coal gasification, devolatilization, or pyrolysis is a very rapid process, occurring almost instantaneously as small coal particles (mean particle size, 2.97×10^{-4} m) are

TABLE 2. ANALYSIS OF KANSAS BITUMINOUS AND ILLINOIS NO. 6 COAL

	Kansas Bituminous	Illinois No. 6
Proximate Analysis (%)		
Fixed carbon (DAF)	55.4	55.47
V.M. (DAF)	44.6	44.53
Ash (Dry)	8.4	2.69
Moisture	7.8	8.40
Ultimate Analysis (% DAF)		
C	75.0	76.91
H	5.3	5.95
N	1.4	1.2
O	10.9	11.71
S	7.5	4.43

fed to a fluidized bed and heated rapidly to the gasification temperature. Anthony and Howard (1976) have investigated this phenomenon in detail and have concluded that the devolatilization of coal apparently depends on such operating conditions as temperature, pressure, particle size, constituents of the carrier gas, type of coal, and heating rate. The decomposition can be accelerated by elevating the temperature. When heated at a more or less conventional rate, coal begins to decompose at 350 to 400°C into a carbon-rich residue and hydrogen-rich volatile fraction. The decomposition continues until a temperature of about 950°C is reached. The volatiles are comprised of various gases and liquids, the relative proportions of which depend on the coal type, the manner and rate of heating, and volatiles residence time. Howell (1979) found that at temperatures above 800 K more than 95% of the proximate volatile matter present in the coal is devolatilized. He used Kansas bituminous coal, the same variety used for the present investigation, with a particle size of 0.42–0.84 mm. He also concluded that an increase in the heating rate accelerates the devolatilization phenomena. Peters et al. (1965) found that rapid heating techniques for coal particles produce more volatiles than traditional slow heating methods.

The devolatilization of coal has been examined by Anthony and Howard (1976) and Howell (1979); they have found that the kinetics can be described by the following equation:

$$1 - y = \frac{V^* - V}{V^*} = \int_0^\infty \exp\left[-\int_0^t k_0 e^{-E/RT}\, dt\right] f(E)dE \quad (1)$$

where

$$f(E) = \frac{\exp\left[-(E - E_m)^2/2\sigma^2\right]}{\sigma(2\pi)^{1/2}} \quad (2)$$

and y is the fraction of the maximum volatile yield.

A plot of fraction of the maximum volatiles yield obtained vs. time, t, at different temperatures for Pittsburgh Seam bituminous coal is shown in Figure 3. The simplification of Eq. 1 and plotting of Figure 3 at different temperatures have been discussed by Howell (1979) and Neogi (1984). It should be noted that the properties of Pittsburgh Seam bituminous coal are very similar to those of Kansas bituminous coal. Normally the gasification temperatures for coal are of the order of 900 K, and the residence time of the solids in a fluidized bed reactor is relatively high, compared to that of the gas. In the light of this, it can be deduced from Figure 3 that temperature is a dominant factor influencing the extent of devolatilization in the reactor. Figure 3 also shows that for temperatures above 900 K, 90% of the devolatilization is complete in less than one second. This naturally gives rise to the assumption that the devolatilization step is instantaneous in a fluidized bed gasifier. This assumption simplifies the model substantially.

Derivation of the Governing Equations

The model assumes a bubble phase and an emulsion phase. The governing equations for the gas in the bubble and emulsion phase and solids in the emulsion phase are presented below. It should be noted that in order to facilitate the numerical solution, the numerical values of the axial dispersion coefficients, D_{ib} and D_{ie}, have been chosen such that they represent nearly plug flow conditions in the bubble phase and nearly completely mixed conditions in the emulsion phase.

A schematic representation of the model is shown in Figure 4.

Gas in bubble phase. A mass balance on species i over an elemental volume of $A_b\Delta x$ in the bubble phase gives:

(Accumulation of species i)
= (rate of species i in by convection) − (rate of species i out by convection)
+ (rate of species i in by dispersion) − (rate of species i out by dispersion)
− (rate of species i out by exchange with the emulsion phase)
+ (rate of production of species i by chemical reaction)

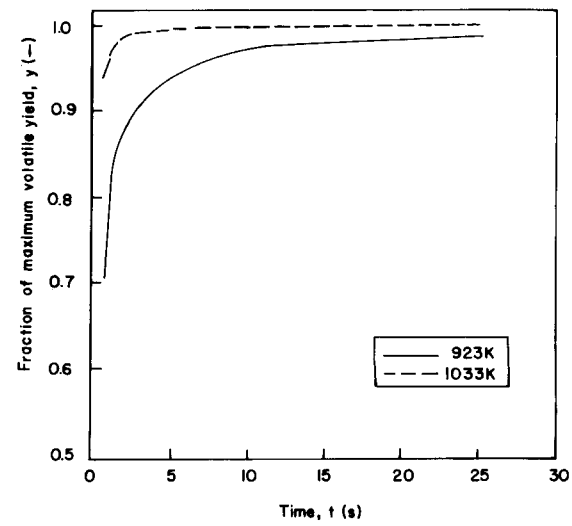

Figure 3. Temperature effect on the rate of devolatilization of coal. E_m = 36.89 kcal/mol, σ = 4.18 kcal/mol, k_o = 2.91 × 10 s^{-1}.

or

$$\frac{\partial}{\partial t}(A_b\Delta x\, C_{ib}) = U_b A_b C_{ib}|_x - U_b A_b C_{ib}|_{x+\Delta x} - D_{ib}A_b \left.\frac{\partial C_{ib}}{\partial x}\right|_x + D_{ib}A_b \left.\frac{\partial C_{ib}}{\partial x}\right|_{x+\Delta x} - A_b\Delta x F_{be}(C_{ib} - C_{ie}) + A_b\Delta x R_{ib} \quad (3)$$

Dividing both sides by $A_b\Delta x$ and letting $\Delta x \to 0$, we obtain

$$\frac{\partial C_{ib}}{\partial t} = -U_b\frac{\partial C_{ib}}{\partial x} + D_{ib}\frac{\partial^2 C_{ib}}{\partial x^2} - F_{be}(C_{ib} - C_{ie}) + R_{ib} \quad (4)$$

Here R_{ib} denotes the rate of generation of gaseous species i by chemical reactions in the bubble phase.

Gas in emulsion phase. Similarly, a mass balance on gaseous species i over an elemental volume of $A_e\Delta x$ in the emulsion phase yields:

$$\frac{\partial}{\partial t}(A_e\Delta x\, \varepsilon_{mf} C_{ie}) = U_e A_e C_{ie}|_x - U_e A_e C_{ie}|_{x+\Delta x} - D_{ie}A_e \left.\frac{\partial C_{ie}}{\partial x}\right|_x + D_{ie}A_e \left.\frac{\partial C_{ie}}{\partial x}\right|_{x+\Delta x} + A_b\Delta x F_{be}(C_{ib} - C_{ie}) + A_e\Delta x\, R_{ie} \quad (5)$$

Dividing both sides of this expression by $A_e\varepsilon_{mf}\Delta x$ and letting $\Delta x \to 0$, we obtain

$$\frac{\partial C_{ie}}{\partial t} = -\frac{U_e}{\varepsilon_{mf}}\frac{\partial C_{ie}}{\partial x} + \frac{D_{ie}}{\varepsilon_{mf}}\frac{\partial^2 C_{ie}}{\partial x^2} + \frac{A_b}{A_e}\frac{F_{be}}{\varepsilon_{mf}}(C_{ib} - C_{ie}) + \frac{R_{ie}}{\varepsilon_{mf}} \quad (6)$$

Here R_{ie} includes the rate of production of gaseous species i by chemical reactions in the emulsion phase as well as a source term for the instantaneous production of species i by the devolatilization step.

Solids in emulsion phase. For the solids in the emulsion phase, C_s is defined as the weight ratio of char with respect to the inert solids in the bed, and B is the total weight of the inerts in the bed. The solid concentration is defined in this manner because the gasification of coal is frequently conducted in a fluidized bed reactor containing an inert matrix. Since the solids are assumed to be completely mixed in the emulsion phase, the material balance on the entire bed yields

$$B\frac{\partial C_s}{\partial t} = (W_{in} - W_{out}) + R_s \quad (7)$$

Here R_s is the rate of consumption of char by the gasification reactions.

The appropriate initial and boundary conditions (for gaseous species in the bubble and emulsion phases, and char as the solid in the emulsion phase) are:

$$t = 0;\ 0 \le x \le H \begin{cases} C_{ib} = C_{io} \\ C_{ie} = C_{io} \\ C_s = 0 \end{cases} \quad (8)$$

$$t > 0;\ x = 0 \begin{cases} C_{ib} - \dfrac{D_{ib}}{U_b}\dfrac{\partial C_{ib}}{\partial x} = C_{io} \\ C_{ie} - \dfrac{D_{ie}}{U_e}\dfrac{\partial C_{ie}}{\partial x} = C_{io} \end{cases} \quad (9)$$

$$t > 0;\ x = H \begin{cases} \dfrac{\partial C_{ib}}{\partial x} = 0 \\ \dfrac{\partial C_{ie}}{\partial x} = 0 \end{cases} \quad (10)$$

where, $i = 1, 2, \ldots, n$, with n representing the total number of gaseous species present in the reactor.

Note that the general governing equations, Eq. 3 through 7, with the initial conditions, Eq. 8, and the boundary conditions, Eq. 9 and 10, may be used to describe various fluidization processes involving chemical reactions with their corresponding rate terms R_{ib}, R_{ie}, and R_s.

In the range of temperature 800–1,200 K and at atmospheric pressure under which coal was gasified, only nine species, CO, CO_2, H_2, H_2O, CH_4, C_2H_6, C_3H_6 ($i = 1, 2, \ldots, 7$, respectively), tar, and char need be considered. Also, the first eight species are the components that have significant concentrations in the volatiles. Since it was assumed that no tar cracking reactions were taking place in the reactor, the total number of differential equations to be solved became 15 (7 for C_{ib}, 7 for C_{ie}, and 1 for char). However, since the char gasification and water-gas shift reactions do not involve C_2H_6 and C_3H_6, the concentration of C_2H_6 and C_3H_6 predicted by the initial devolatilization data was simply added to the final gas concentration. This reduced the number of PDE to 11. It should be noted that the boundary conditions of the model preclude any chemical reactions taking place in the freeboard of the reactor, as stated in the initial assumptions for the model development. Although the secondary reactions involving tar cracking are not included in the model, an initial yield of heavy volatiles and its distribution are considered.

The expressions for the rate terms are

$$R_{1b} = R_{4b} = -R_b \quad (11)$$

$$R_{2b} = R_{3b} = R_b \quad (12)$$

$$R_{5b} = 0 \quad (13)$$

$$R_{1e} = S\left(k_1 C_{4e} + \frac{k_2 C_{2e}}{2}\right) - R_{sr} + C_g C_1 \quad (14)$$

$$R_{2e} = -S(k_2 C_{2e}) + R_{sr} + C_g C_2 \quad (15)$$

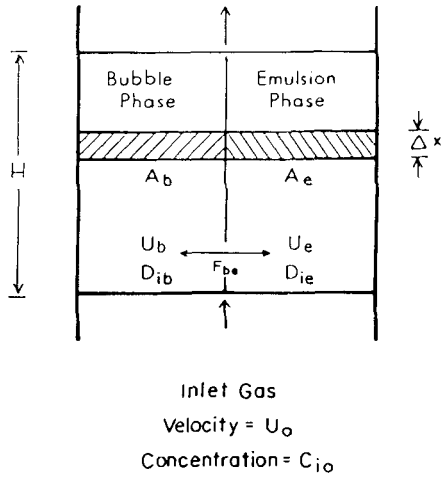

Figure 4. Schematic representation of the model.

$$R_{3e} = S(k_1C_{4e} - k_3C_{3e}) + R_{sr} + C_gC_3 \quad (16)$$

$$R_{4e} = -Sk_1C_{4e} - R_{sr} + C_gC_4 \quad (17)$$

$$R_{5e} = \frac{1}{2}(Sk_3C_{3e}) + C_gC_5 \quad (18)$$

$$R_s = -\left(k_1C_{4e} + k_2C_{2e} + \frac{k_3C_{3e}}{2}\right)B\,A_cC_sM_c \quad (19)$$

where

$$R_b = k_4C_{1b}C_{4b} - k_5C_{2b}C_{3b} \quad (20)$$

$$C_g = \frac{F}{HA(1-\delta)} \quad (21)$$

$$S = \frac{B\,A_cC_sC_c}{HA(1-\delta)} \quad (22)$$

$$R_{sr} = k_4C_{1e}C_{4e} - k_5C_{2e}C_{3e} \quad (23)$$

Hydrodynamic Relationships

Hydrodynamics of the bubbling phenomenon interrelates the variables involved in this model. Functional relationships among the parameters and variables that depend on the hydrodynamics of the fluid bed are given below.

1. The bubble diameter, d_b, is estimated using Mori and Wen's (1975) correlation:

$$d_b = D_{bm} - (D_{bm} - D_{bo})\exp(-0.3\,x/D)$$

$$D_{bm} = 0.652\,\{A(U_o - U_{mf})\}^{0.4}$$

$$D_{bo} = 0.00376(U_o - U_{mf})^2$$

where D_{bo} is the initial bubble diameter, and D_{bm} is the maximum bubble diameter. The equivalent bubble diameter, d_b, (Kunii and Levenspiel, 1969) is calculated at the middle of the total bed height, $x = H/2$.

2. The bubble velocity, U_b, is calculated by using the correlation proposed by Davidson and Harrison (1963):

$$U_b = (U_o - U_{mf}) + 0.711\,(gD_b)^{0.5}$$

3. The volume fraction of bubble phase, δ, is calculated from

$$\delta = (U_o - U_{mf})/U_b$$

4. The emulsion phase gas velocity, U_e, is calculated as

$$U_e = U_{mf}/(1-\delta)$$

5. The gas-exchange coefficient between bubble and emulsion phases, F_{be}, is calculated from the following correlation proposed by Kobayashi and Arai (1967):

$$F_{be} = 0.11/D_b$$

6. The height of the expanded bed, H, is calculated iteratively from the material balance on the solid as

$$H = H_{mf}/(1-\delta)$$

Additional Assumptions Imposed in Simulation of Coal Gasification Process

To illustrate the application of the present model, the gasification of coal in our experimental fluidized bed gasifier has been simulted. Additional assumptions made for the simulation are:

1. The fraction of char and total volatiles generated in the devolatilization step are the same as those obtained from thermogravimetric studies. Data obtained by Howell (1979) were used and are presented in Table 3.

2. The fractions of liquid and gas in the total volatiles generated as well as the initial composition of the gas, were taken from the results obtained by Yeboah et al. (1980). The initial product distribution and the initial gas composition are presented in Table 3.

3. Adjustments were made on the kinetic parameters involving coal char obtained by Biba et al. (1978). This was done to incorporate the fast rate of char gasification indicated by our experimental observations. The adjusted parameters, listed in Table 4, were used for the simulation. The kinetic parameters of the shift reaction have the values reported by Biba et al. (1978) and by Yoon (1977).

The second assumption is made because no devolatilization data on Kansas bituminous coal is available. The proximate and ultimate analyses of both types of coal are very similar, as shown in Table 2. Yeboah et al. (1980) performed pyrolysis experiments on Illinois No. 6 coal with sand or calcined dolomite as the bed material. They concluded that secondary reactions are enhanced by dolomite stones. The data used in the present

TABLE 3. DEVOLATILIZATION PRODUCT DISTRIBUTION FOR COAL

Product	Temperature, K					Data Source
	873*	923	973*	1,033	1,073*	
Char (wt. % DAF)	60.0	62.6	64.0	65.1	65.2	TGA experiment
Volatiles (wt. % DAF)	40.0	37.4	36.0	34.9	34.8	Howell (1979)
Volatiles composition (wt. % DAF)						
Dry gas	13.0	14.2	14.8	15.0	15.1	Yeboah et al. (1980)
Tar	16.6	17.0	16.4	15.0	13.8	Yeboah et al. (1980)
Water	10.4	6.2	4.8	4.9	5.9	Yeboah et al. (1980)
Dry gas composition (vol. %)						
CO	12.5	14.1	15.5	17.0	17.9	Yeboah et al. (1980)
CO_2	15.0	13.7	13.0	12.0	17.9	Yeboah et al. (1980)
H_2	37.1	39.8	41.6	42.8	43.6	Yeboah et al. (1980)
CH_4	21.8	20.5	19.1	17.5	16.8	Yeboah et al. (1980)
C_2H_6	4.1	3.8	3.3	2.9	2.6	Yeboah et al. (1980)
C_3H_6	3.6	3.5	3.0	2.8	2.3	Yeboah et al. (1980)
Others**	5.9	4.6	4.5	4.1	4.0	Yeboah et al. (1980)
Avg. mol. wt.	19.67	18.7	18.07	17.9	17.71	Yeboah et al. (1980)

*Extrapolated and interpolated data.
**C_2H_4, C_3H_8

TABLE 4. KINETIC PARAMETERS FOR THE REACTIONS

Reactions	Activation Energy* (E_j) kJ/kmol	Adjusted Frequency Factor** (k_j^o), m/h
$C + H_2O \xrightarrow{k1} CO + H_2$	121,417	3.0×10^2
$C + CO_2 \xrightarrow{k2} 2CO$	360,065	2×10^7
$C + 2H_2 \xrightarrow{k3} CH_4$	230,274	750.0
$CO + H_2O \xrightarrow{k4} CO_2 + H_2$	12,560	0.1×10^8(m³/kmol · h)
$CO + H_2O \underset{k5}{\overset{k4}{\rightleftharpoons}} CO_2 + H_2$	$K_w = \frac{k_4}{k_5} = 0.0265 \exp(3955.7/T)$*	

* Yoon (1977).
** $k_j = k_j^o \exp(-E_j/RT)$.

study were those of the pyrolysis performed by Yeboah et al. in an inert atmosphere using sand as the bed material. Since in this case no enhanced secondary reactions are expected to occur, it is reasonable to assume that the product distribution reported by Yeboah et al. corresponds directly to the primary devolatilization reaction.

METHOD OF NUMERICAL SOLUTION

There are eleven nonlinear partial differential equations (PDE) that need be solved for simulation of the gasifier. The simultaneous solution of these parabolic partial differential equations yields the transient concentration distributions of the different species in the reactor. The numerical solution of these nonlinear PDE's is often complicated and time-consuming. Sincovec and Madsen (1975) have developed a software interface that overcomes the difficulties associated with solving stiff and nonstiff nonlinear parabolic PDE's. It has been employed to numerically solve the governing equations of the model. The package uses the "method of lines" technique for spatial discretization to convert the nonlinear partial differential equations into a system of time-dependent, nonlinear, ordinary differential equations. Gear's backward difference formulas are then used for the time integration. A modified Newton's method with an internally generated Jacobian matrix is used to solve the nonlinear equations. For each calculation, the subroutine automatically adjusts the time step size to achieve a specified error level.

A flow diagram of the computational procedure based on the present model is given in Figure 5. The relative error bound for the time integration process is set at 10^{-3} and the number of spatial meshes specified for this study is 11. It should be noted that the dynamic solutions of the system include the steady state solutions as the limit.

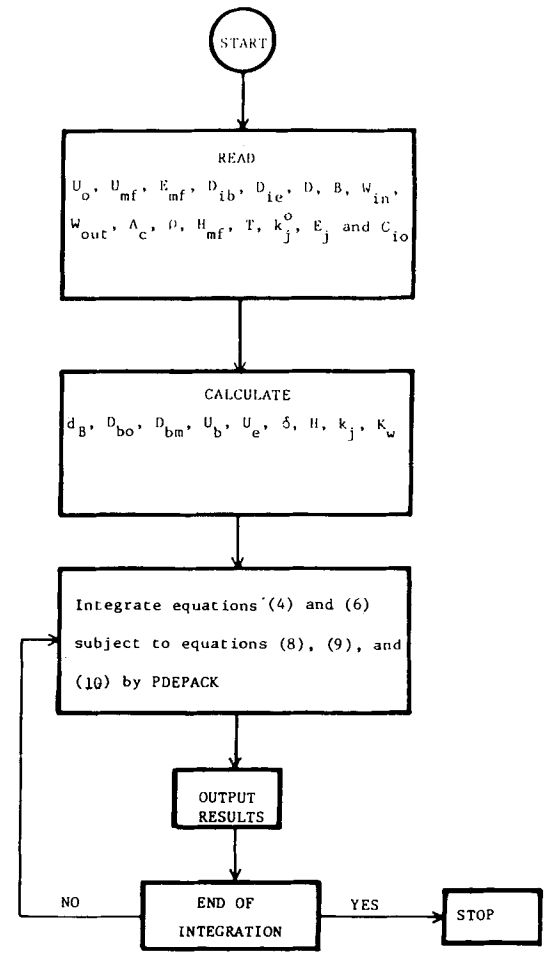

Figure 5. Flow diagram of the computation.

RESULTS AND DISCUSSION

The experimentally observed effect of temperature on the composition of the product gas is shown in Figure 6. Sixty-six data points for each component are shown in these figures. The total product gas mass yield as a function of temperature is plotted in Figure 7. The lines in each figure represent simultaneous regression analysis of the data. Experimentally determined mass yields of the major components of the product gas at different temperatures are presented in Table 5.

The concentration of H_2 increased with temperature and ranged from 51.1% at 873 K to 60.0% at 1,073 K. Carbon dioxide increased from 25.0% at 873 K to 30.5% at 923 K and then decreased to 16.0% at 1,073 K. Methane decreased slightly with temperature, ranging from 11.1% at 873 K to 2.9% at 1,073 K. The minor components, C_2H_4, C_2H_6, C_3H_6, and C_3H_8,

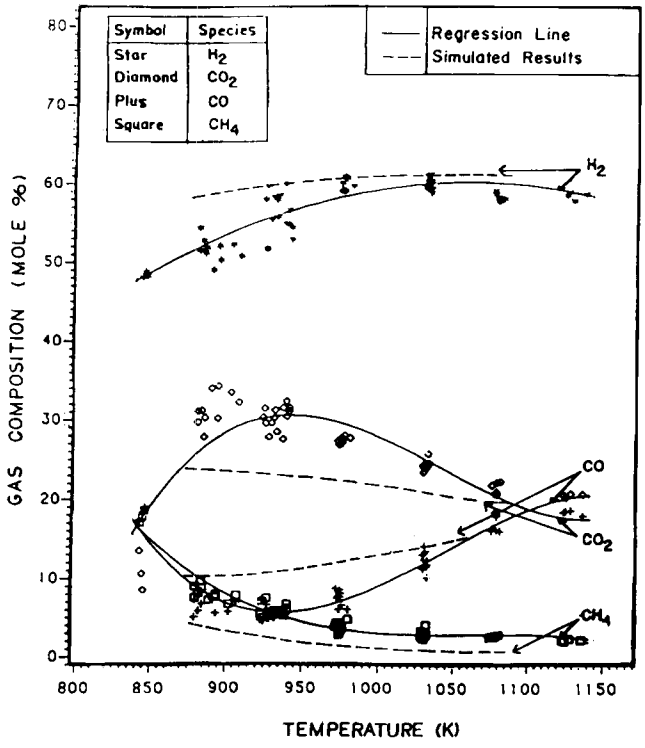

Figure 6. Experimental and simulated results: effect of temperature on the product gas composition (major components).

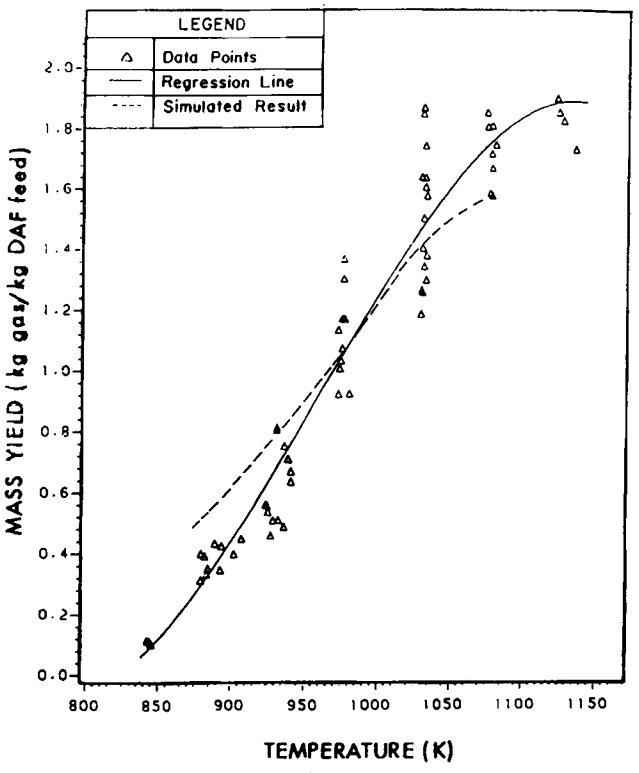

Figure 7. Experimental and simulated results: effect of temperature on the product gas mass yield.

all decreased in concentration with an increase in temperature; their combined composition represented less than 3–4% of the total gas yield.

The mass yield of the product gas increased from 0.12 kg gas/kg DAF feed at 850 K to 1.88 kg gas/kg DAF feed at 1,150 K. Gas mass yields greater than 1.0 kg gas/kg DAF feed were obtained at temperatures greater than 970 K (Figure 7). These high yields were simply due to steam becoming a part of the produced gas through water-gas shift and char gasification reactions. These reactions were enhanced because of the large amount of excess steam in the present experimental system. Moreover, the small size of the char particles made them highly reactive. The experimental data indicate that the water-gas shift and char gasification reactions were the major factors influencing the gas composition and mass yield; the extent of these reactions increased as the temperature increased. It was also

TABLE 5. COMPARISON OF EXPERIMENTAL AND SIMULATED STEADY STATE RESULTS

Gas Components mol %	Temperature, K									
	873		923		973		1,033		1,073	
	Expt.	Simul.	Expt.	Simul.	Expt.	Simul.	Expt.	Simul.	Expt.	Simul.
CO	10.01	10.40	6.00	11.75	7.34	13.53	12.40	15.49	15.83	16.59
CO_2	25.02	24.28	30.50	23.99	29.71	23.19	24.00	22.06	21.01	21.48
H_2	51.10	57.87	55.10	59.45	57.50	59.94	59.40	59.84	60.01	59.51
CH_4	11.11	4.41	6.20	2.92	4.10	2.04	3.10	1.60	2.90	1.51
C_2H_6	1.01	0.90	0.40	0.59	0.20	0.39	0.10	0.29	0.15	0.26
C_3H_6	0.73	0.79	0.42	0.54	0.22	0.35	0.10	0.28	0.00	0.23
Others*	1.10	1.31	1.40	0.72	0.78	0.53	0.60	0.41	0.15	0.40
Mass Yield of Gas (kg gas/kg DAF feed)	0.34	0.51	0.66	0.78	1.08	1.15	1.50	1.40	1.73	1.43
Mass Yields of Individual Gas Components (kg gas/kg DAF feed)										
CO	0.04	0.089	0.05	0.158	0.17	0.273	0.35	0.380	0.46	0.414
CO_2	0.24	0.327	0.52	0.510	0.75	0.736	0.94	0.850	1.06	0.850
H_2	0.03	0.035	0.05	0.057	0.08	0.086	0.11	0.105	0.12	0.106
CH_4	0.02	0.022	0.03	0.022	0.03	0.023	0.04	0.022	0.03	0.022

*C_2H_4, C_3H_8

observed that the extent of tar cracking reactions increased with temperature. Note that the gas phase residence time in the reactor was found to be of the order of 4–7 s. Our previous results involving biomass gasification indicated that a residence time of this order is sufficient for the cracking reaction to reach completion at a given temperature (Singh, 1983). Visual observation of the color of the condensate obtained in the experiments also suggested that the tar production decreases with increasing temperature and becomes almost insignificant at 930–950 K. Tyler (1979) conducted experiments on flash pyrolysis of a variety of coal in a fluidized bed reactor. His study showed that tar yield decreased from 20–30% w/w DAF coal to 8–12% w/w DAF coal as the temperature increased from 873 to 1,173 K. He also concluded that the presence of char in the bed reduces the tar yield and attributed this not to cracking reactions but to polymerization reactions occurring within the bed. Present experimental investigation suggests substantial tar cracking reaction, but one should note that a part of the tar produced may have participated in polymerization reaction, since there was char holdup in the bed.

The gas chromatograph reading of the product gas compositions approached steady state within 20–25 min after the initiation of feeding in the reactor. The elutriation rate of char and the amount of char accumulated in the bed were observed to reach steady state values within 30 to 40 min. The observed steady state carbon conversion increased from 7% at 850 K to 82% at 1,125 K. The carbon conversion was estimated to be 80% at 1,050 K from the steady state char output. This overestimated the carbon conversion in light of the holdup of char in the system.

Figures 8 and 9 present the simulated transient dry product gas compositions for temperatures of 923 and 1,033 K, respectively. Since transient experimental data were not obtained, only the steady state product gas compositions and mass yields predicted by the model are compared with the experimental observations in Table 5 and Figures 6 and 7. Note that the simulated gas compositions and mass yields are in reasonably good agreement with the experimental results in the temperature range presented. However, as can be seen from Table 5 and Figures 6 and 8, there are some discrepancies between the simulated and experimental data. They can be explained

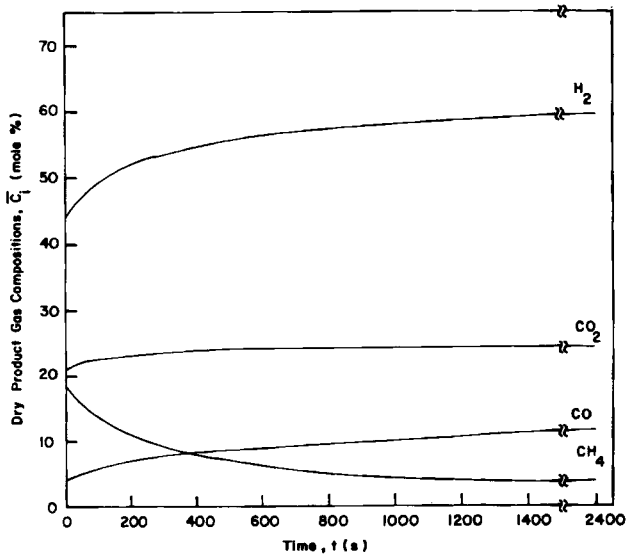

Figure 8. Simulated result: transient dry product gas composition at T = 923 K.

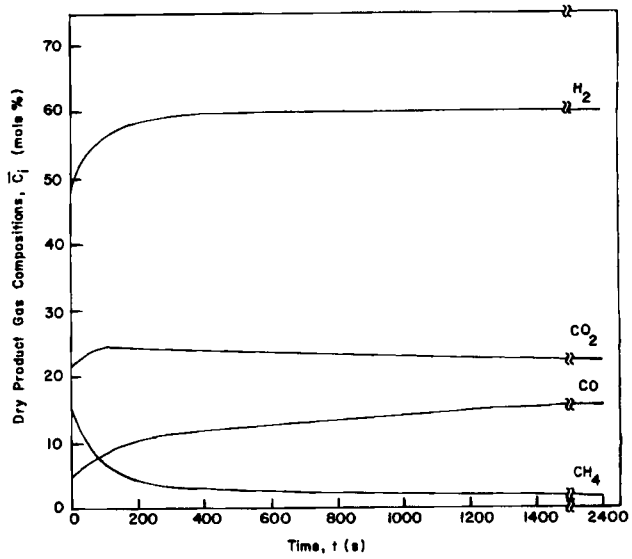

Figure 9. Simulated result: transient dry product gas composition at T = 1,033 K.

by the fact that secondary reactions involving tar cracking and freeboard reactions are not included in the model.

For the preliminary simulations, the rate constants given by Biba et al. (1978) for char gasification reactions were used since the corresponding data were not available for Kansas bituminous coal. It was found that the model predicted negligible char gasification reactions. Since char gasification was extensive in our experiments, it was concluded that the kinetic parameters proposed by Biba et al. (1978) did not represent appropriate values for the coal under investigation. The experimentally determined frequency factors cited in the literature are strictly dependent on the type of coal, specific surface area, and corresponding values of the activation energy. It should be noted that Biba et al. (1978) used coal with a particle size of the order of 2 cm, whereas the average coal particle size used in the present work was only 0.03 cm. Due to attrition in the bed, the char particles probably became even smaller, resulting in an order of magnitude increase in their reactivity. It was therefore necessary to select a suitable set of parameters for the specific coal under investigation. Sensitivity studies of the model simulation results were conducted using different values of the frequency factor for the char gasification reactions. The resulting gas composition and mass yields were compared with the corresponding experimental values at a particular temperature. This sensitivity analysis yielded the frequency factors employed in the present simulation (Table 4). It should be noted that the rate constants used for the simulations predict trends that are consistent with the experimental observations, especially in view of the complexity of the overall system and the mathematical model.

Factors that are not taken into account in deriving the model include the effects of the residence time of the volatiles in the freeboard and tar cracking. Recall that the residence time of the volatiles was found to be 4–7 s in the experimental system. This long residence time will enhance tar cracking and gas phase reactions in the freeboard, as well as increase the extent of water-gas shift reaction, thus producing additional CO_2 and H_2. A comprehensive simulation should include the cracking reactions involving the heavy volatiles and their time-temperature history in both the fluidized bed and the freeboard. The experimental results suggest significant tar cracking at temperatures below 940 K. Since tar contributes 15–16 wt. % of

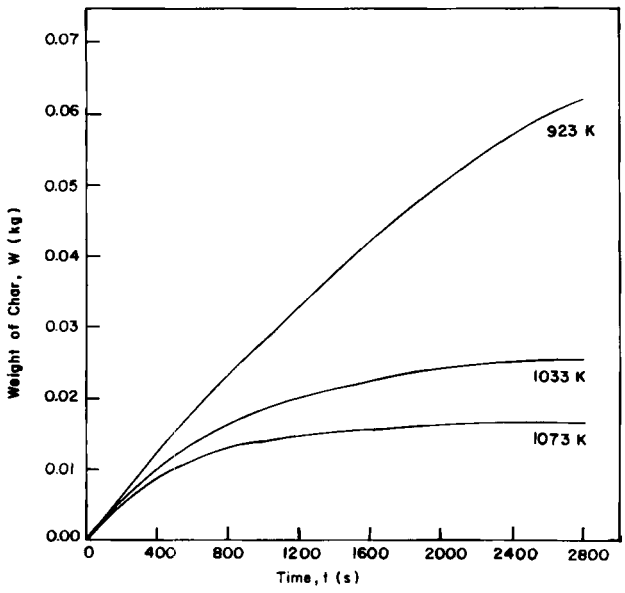

Figure 10. Simulated result: weight of char produced as a function of time.

the initial feed, the tar cracking reactions should be incorporated in refining the model.

The simulated char content of the bed increases with time as shown in Figure 10. Notice that the amount of char accumulated in the bed approaches a steady value faster at higher temperatures (1,033 and 1,073 K) than at a lower temperature (923 K). Furthermore, a greater amount of char accumulates in the bed at the lower temperature. This is expected since the extent of the char gasification reactions increases with an

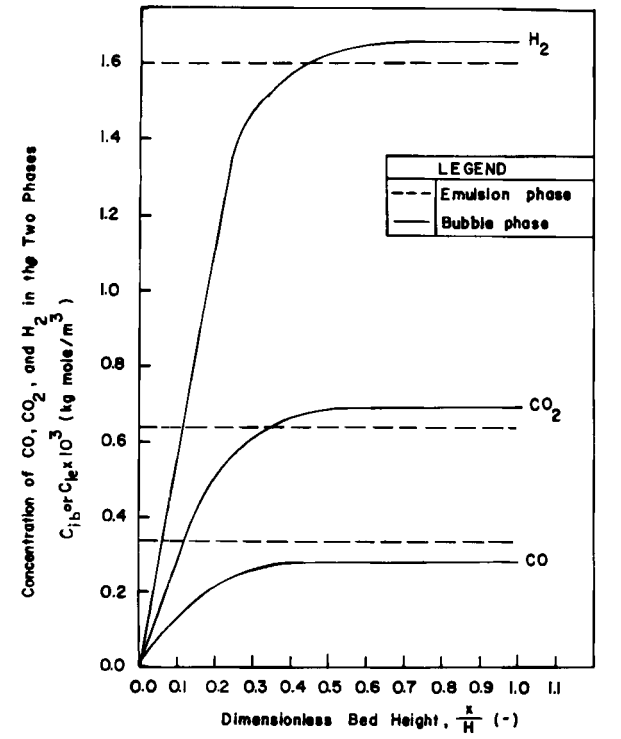

Figure 11. Simulated result: steady state axial concentration profiles of CO, CO_2, and H_2 at T = 923 K.

increase in the temperature. As mentioned earlier, the weight of the char observed in the bed reached a steady value 30–40 min after the initiation of feed in the experiments. The foregoing discussion further substantiates that the proposed model simulates the trends observed in the experimental system.

The axial concentration profiles predicted by the simulation are shown in Figure 11 for the major gas components (H_2, CO, and CO_2) in both the bubble and emulsion phases. It can be seen that the concentrations of H_2, CO, and CO_2 in the bubble phase increase with the bed height and that each component approaches its concentration in the emulsion phase before exiting from the top of the bed. This implies intensive interphase mixing between the emulsion and bubble phases under the operating conditions simulated. Also, inspection of the transient solutions (Figures 8 and 9) shows that the gas composition reaches steady state in about 1,400–1,600 s, thus agreeing well with the experimental observations.

To implement the present model in practice, three refinements need to be made in specific areas. The first involves the inclusion of the reactions of heavy volatiles. To do so requires the following information: (1) knowledge of the molecular species present in the heavy volatiles and their distribution, (2) kinetics of their cracking reactions, and (3) knowledge of the time-temperature history of the volatiles. The second entails improvement of the initial conditions of the model pertaining to the initial devolatilization and of the rate constants for the gasification reactions. To achieve this, the initial product distribution and kinetic rate constants for the char formed from the coal of interest are needed. The third requires incorporation of the freeboard reactions in the model.

ACKNOWLEDGMENT

This work was conducted under the sponsorship of the Engineering Experiment Station (Hydrogen Project) of Kansas State University.

NOTATION

A = cross-sectional area of the reactor, m^2
A_b = cross-sectional area of the reactor occupied by the bubble phase, m^2
A_e = cross-sectional area of the reactor occupied by the emulsion phase, m^2
A_c = surface area of char, m^2/kg
B = weight of the inert solids in the reactor, kg
C_c = weight fraction of carbon in char
C_i = yield of the ith species by devolatilization, kmol/kg of DAF feed
$\overline{C}_i$ = molar concentration of the ith species exiting from the bed, mol %
C_{ib} = concentration of the ith species in the bubble phase, kmol/m^3
C_{ie} = concentration of the ith species in the emulsion phase, kmol/m^3
C_{io} = initial or inlet concentration of the ith species, kmol/m^3
C_s = concentration of char in the emulsion phase, kg char/kg inert solids
C_g = dry ash free feed rate per unit volume of the emulsion phase, kg/m^3
D = diameter of the reactor, m
D_{ib} = axial dispersion coefficient through the bubble phase, m^2/s

D_{ie} = axial dispersion coefficient through the emulsion phase, m^2/s
d_b = bubble diameter, m
D_{bm} = maximum bubble diameter, m
D_{bo} = initial bubble diameter, m
E = activation energy, kcal/gmol
E_m = mean activation energy, kcal/gmol
F = dry ash free feed rate of coal, kg/s
F_{be} = gas interchange coefficient between the bubble and emulsion phases based on the volume of bubbles, 1/s
$f(E)$ = activation energy distribution
H = bed height, m
H_{mf} = bed height at minimum fluidization, m
k_o = frequency factor, 1/s
k_j = rate constant for the jth reaction, 1/s
$f(E)$ = activation energy distribution
K_w = equilibrium constant for the water-gas shift reaction
M_c = atomic weight of carbon, 12 kg/kmol
R = gas constant = 1.987 kcal/kmol · K
R_b = variable defined by Eq. 20, kmol/m³ · s
R_{ib} = rate of generation of the ith species in the bubble phase based on the volume of bubbles, kmol/m³ · s
R_{ie} = rate of generation of the ith species in the emulsion phase based on the volume of the emulsion phase, kmol/m³ · s
R_s = rate of consumption of char in the emulsion phase, kg/s
R_{sr} = variable defined by Eq. 23, kmol/m³ · s
S = variable defined by Eq. 22, m^2/m^3
t = time, s
T = temperature, K
U_b = bubble rise velocity, m/s
U_e = superficial velocity of emulsion gas based on the emulsion phase cross-sectional area, m/s
U_{mf} = superficial velocity of gas at minimum fluidization, m/s
V^* = proximate volatile matter, %
V = volatile matter yield, %
W_{in} = rate of char into the reactor generated by the devolatilization of coal, kg/s
W_{out} = rate of char out of the reactor, kg/s
x = axial distance from the distributor, m
y = fraction of maximum volatile yield

Subscripts

i = indices specifying species (1 = CO; 2 = CO_2; 3 = H_2; 4 = H_2O; 5 = CH_4)
j = indices indicating the reactions

Greek Letters

δ = volume fraction of the bubble phase
ρ = density of the solids in the reactor, kg/m³
σ = standard deviation from mean activation energy, kcal/gmol
ε_{mf} = void fraction in the bed at minimum fluidization

LITERATURE

Anthony, D. B., and J. B. Howard, "Coal Devolatilization and Hydrogasification," *AIChE J.*, **22**(4), 625 (1976).
Becker, H. A., J. M. Beer, and B. M. Gibbs, "A Model for Fluidized-Bed Combustion of Coal," *Inst. Fuel Symp. Ser. No. 1: Fluidized Combustion, Proc.*, **1**, A1-1 (1975).
Biba, V., et al., "Mathematical Model for the Gasification of Coal under Pressure," *Ind. Eng. Chem. Proc. Des. Dev.*, **17**, 92 (1978).
Chang, C. C., L. T. Fan, and W. P. Walawender, "Dynamic Modeling of Biomass Gasification in a Fluidized Bed," *AIChE Symp. Ser.*, **80** (234), 80 (1984).
Davidson, J. F., and D. Harrison, *Fluidized Particles*, Cambridge University Press, New York, pp. 19 and 21 (1963).
Howell, J. A., "Kansas Coal Gasification," M.S. Thesis, Kansas State University (1979).
Kato, K., and C. Y. Wen, "Bubble Assemblage Model for Fluidized Bed Catalytic Reactors," *Chem. Eng. Sci.*, **24**, 1,351 (1969).
Kobayashi, H., and F. Arai, "Determination of Gas Cross-Flow Coefficient between the Bubble and Emulsion Phases by Measuring the Residence Time Distribution of Fluid in a Fluidized Bed," *Kagaku Kogaku*, **31**, 239 (1967).
Kunii, D., and O. Levenspiel, *Fluidization Engineering*, Wiley, New York, 108–139 (1969).
Mori, S., and C. Y. Wen, "Estimation of Bubble Diameter in Gaseous Fluidized Beds," *AIChE J.*, **21**, 109 (1975).
Neogi, D., "Coal Gasification in an Experimental Fluidized Bed Reactor," M.S. Thesis in Chemical Engineering, Kansas State University (1984).
Peters, W., and H. Bertling, "Kinetics of the Rapid Degasification of Coals," *Fuel*, **44**, 317 (1965).
Raman, K. P., et al., "Mathematical Model for the Fluid-Bed Gasification of Biomass Materials. Application to Feedlot Manure," *Ind. Eng. Chem. Proc. Des. Dev.*, **20**, 686 (1981).
Sincovec, R. F., and N. K. Madsen, "Software for Nonlinear Partial Differential Equations," *ACM Trans. Math. Software*, **1**, 232 (1975).
Singh, S. K., "The Gasification of Biomass in a Fluidized Bed Reactor," M.S. Thesis in Chemical Engineering, Kansas State University (1983).
Tyler, R., "Flash Pyrolysis of Coals: Devolatilization of Bituminous Coals in a Small Fluidized-Bed Reactor," Report MRB/179, CSIRO Division of Process Technology, North Ryde, N.S.W., Australia (1979).
Walawender, W. P., S. Ganesan, and L. T. Fan, "Steam Gasification of Manure in a Fluid Bed: Influence of Limestone as a Bed Additive," *Energy from Biomass and Wastes V*, Inst. Gas Tech., pp. 517–527 (1981).
Yeboah, Y. D., et al., "Effects of Calcined Dolomite on the Fluidized Bed Pyrolysis of Coal," *Ind. and Eng. Chem. Proc. Des. Dev.*, **19**, 646 (1980).
Yoon, H., J. Wei, and M. M. Denn, "Modeling and Analysis of Moving Bed Coal Gasifiers," AF-590, Vol. 1, Technical Planning Study 76-653, Research Project 986-1, Final Report, (Nov., 1977).
Zeles, S. R., "Mathematical Model for Fluidized Bed Coal Gasification Reactors," M. S. Thesis, Massachusetts Institute of Technology, (1978).

Manuscript received July 17, 1984, and revision received Mar. 22, 1985.